Spectroscopy of Hydrothermal Reactions 13. Kinetics and Mechanisms of Decarboxylation of Acetic Acid Derivatives at 100−260 °C under 275 bar

A. J. Belsky, P. G. Maiella, and T. B. Brill*

Department of Chemistry and Biochemistry, University of Delaware, Newark, Delaware 19716

Received: October 22, 1998; In Final Form: February 4, 1999

The rates and pathways of decarboxylation of acetic acid derivatives, RCO_2H, and their Na^+ salts, RCO_2Na, which possess electron-withdrawing groups (R = CCl_3-, CF_3-, $HOC(O)CH_2-$, $NH_2C(O)CH_2-$, CF_3CH_2-, $NCCH_2-$, $CH_3C(O)-$) were determined in H_2O at 100−260 °C and a pressure of 275 bar. Simple conversion to RH + CO_2 occurs in most cases, except that H_2O appears to be a required reactant for the anions. Real-time FTIR spectroscopy was used to determine the rate of formation of CO_2 in flow reactors constructed of 316 stainless steel (SS) and of titanium. With a few exceptions, the rate of decarboxylation is similar within the 95% confidence interval in 316 SS and Ti and the difference is smaller than that caused by R. Therefore, while wall effects/catalysis may exist in some cases, it plays a lesser role in the relative rates than the substituent R. The acid form of the keto derivatives decarboxylates more rapidly than the anionic form, whereas the reverse is true for the nonketo derivatives. In keeping with the greater role of H_2O as a reactant, the entropy of activation for the anions is smaller or more negative than for the acids. A Taft plot of the decarboxylation rates suggests that the mechanistic details can be interpreted in terms of the various roles of R. Where R = $HOC(O)CH_2-$ and $NH_2C(O)CH_2-$, decarboxylation occurs faster than expected, probably because a cyclic transition state can exist. The rate is slower than expected for R = CF_3-, perhaps because of stabilization of the acid by hyperconjugation. The mechanism of decarboxylation of acids of the remaining R groups is similar and the steric effect of R is somewhat more influential than its electron withdrawing power.

Introduction

The carboxylate group is among the most important chemical entities in a variety of natural settings including oil field brines[1] and hydrothermal vents in the crust of the earth.[2] Carboxylic acids are also frequent intermediates in the degradation of organic compounds by aqueous oxidative processes, such as supercritical water oxidation[3] and wet air oxidation.[4] The common ground in all of these cases is the presence of organic molecules in an aqueous phase at high pressures and temperatures. Although much is known about the thermodynamics of carboxylic acids in H_2O,[5] most previous kinetic studies in the hydrothermal medium have been directed at the simplest acids in the series—formic[6,7] and acetic.[8,9] The behavior of other derivatives has not been determined as deeply.

A rather general decomposition reaction of carboxylic acids in H_2O solution appears to the decarboxylation reaction 1.

$$RCO_2H \rightarrow RH + CO_2 \qquad (1)$$

This reaction is among the more important steps in the carbon cycle of animal systems,[10] and contributes to the relative concentrations of various carboxylic acids in subterranean H_2O solutions.[11] In the latter case, acetic acid occurs in concentrations up to about 10^4 ppm in oil field brine owing to its thermodynamic stability[12] and kinetic inertness[13] toward reaction 1. Other carboxylic acids occur in the same environment but with lower concentrations.

Reaction 1 is described by a first-order rate expression in H_2O,[6,7,14−16] but owing to the probable association between the acid and H_2O during the reaction, a pseudo-first-order expression is perhaps a better description. In fact, several mechanisms for reaction 1 appear to exist that depend on the identity of R. When R = CH_3, very large differences in the rate are observed on different substrate surfaces.[8,11] For example, the half-life of acetic acid at 100 °C is about a factor of 3×10^{14} larger in the presence of titanium compared to stainless steel.[11] The rate of reaction 1 for R = H at hydrothermal conditions was recently found to depend significantly on the material of construction of the reactor,[6] although it has also been interpreted as being a homogeneous reaction.[7] It has been generally concluded[8] that decarboxylation of monocarboxylic acids is catalyzed by the reactor surface, but the R groups on which these data are based are primarily electron-donating.

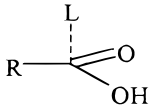

(I)

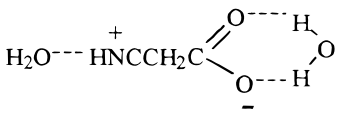

(II)

In addition to possible control of the rate by the reactor wall or substrate, a second factor in promoting reaction 1 was emphasized by Clark[10] who proposed that a nucleophile, L, can associate with the electropositive carbon atom of the carbonyl group (structure I), weaken the R−C bond, and facilitate liberation of CO_2. A variation on this mechanism was proposed when R = $-CH_2CN$ based on MO computations at the AM1 level with several H_2O molecules in the transition state (structure II).[17] The association of the zwitterion with two H_2O molecules as shown in structure II was proposed to be the lowest energy transition state on the way to decarboxylation. Dicarboxylic and other β-keto acids that are capable of forming the cyclic transition state III are also well-known to decarboxylate readily.[13,16,18,19] Structure III is shown for malonic acid, but

* Corresponding author. brill@udel.edu.

10.1021/jp984122d CCC: $18.00
Published on Web 05/05/1999

malonic acid is also known to decarboxylate even more readily in the presence of L.[20] Hence some combination of structures I and III has been proposed in this case.[10]

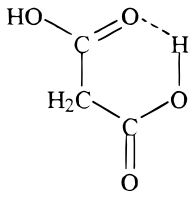

(III)

It is suggested by the examples above that various decarboxylation reaction mechanisms may exist for simple carboxylic acids in H_2O solution. The balance of competing mechanisms appears to depend mainly on the specifics of R. When R is electron-neutral or -donating,[6,8,9] the acid is more inert and the rate of reaction 1 has been observed to depend significantly on the reactor surface. On the other hand, a systematic study of the effect of electron-withdrawing R groups on the rate of reaction 1 has not been reported at hydrothermal conditions and is the subject of this article. The present work differs somewhat from many previous decarboxylation reaction studies in that real-time spectroscopic measurements of concentrations are obtained in the initial 30 s of reaction by the use of an infrared spectroscopy cell-flow reactor. The results reveal that the dependence of the rate of reaction 1 on R is not a simple one, but is more a function of the characteristics of R than the reactor type.

Experimental Section

The flow reactor/spectroscopy cells used for this work have been described in earlier papers.[21,22] The essential feature is that a flat duct is created by compressing a gold-foil washer between the cell body and flange made of either 316 stainless steel (SS) or grade 2 titanium. The flat duct contains the entrance and exit flow tubes and two sapphire windows. The thickness of the duct is determined by the thickness of the gold foil and defines the path length between the sapphire windows. The path length was determined precisely by the absorbance of a known amount of CO_2[23] and was $25-35 \pm 1$ μm. The path length did not change with temperature. The surface-to-volume ratio in these cells was $20-50$ cm^{-1}. The volume of the cell was calculated in each case because it was needed to determine the residence time.

The choice of the two reactor types (316 SS and Ti) was made, in part, to test the role of surface catalysis on the reaction rate. The half-life for decarboxylation of CH_3CO_2H differs by about 10^7 at 100 °C on SS and Ti surfaces,[11] and, therefore, these cell materials should give an indication of the importance of surface effects on the decarboxylation of the derivatives of acetic acid. We recognize that a preferred method of testing the role of surface catalysis is to vary the surface-to-volume ratio. This method is not practical in the precision spectroscopy flow reactors used in this work. We also recognize that the present study is not a decisive surface study particularly because the cell surfaces are machined and also undoubtedly possess an undefined degree of oxidation.

The controls on the system for obtaining the temperature (±1 °C), pressure (±1 bar), and volume flow rate (0.054−1.00 mL/min) have been discussed and modeled.[21,22,24] These parameters were monitored, controlled, and recorded with a Visual Basic program. The temperature range used for the kinetics measurements in this paper was 100−260 °C at a constant pressure of 275 bar. The density of H_2O changes somewhat under these conditions ($\rho_{100\,°C} = 0.971$ g/cm^3; $\rho_{260\,°C} = 0.813$ g/cm^3), but is sufficiently high to assume that the properties of liquid H_2O are retained. A correction for the fluid density was made in the IR spectral intensity at each temperature. The true residence times of the reacting fluid were calculated by dividing the internal volume (entrance tube and flat duct) by the mass flow rate (volume flow rate × ρ_T).

The acids whose decarboxylation rates were determined in this study were mostly available commercially: cyanoacetic, $NCCH_2CO_2H$; trichloroacetic, CCl_3CO_2H; trifluoroacetic, CF_3CO_2H; pyruvic, $CH_3C(O)CO_2H$ (Aldrich); trifluoropropionic, $CF_3CH_2CO_2H$ (Indofine). Malonamic acid, $NH_2C(O)CH_2CO_2H$, was prepared as described elsewhere.[25] Kinetic data for malonic acid,[16] $HOC(O)CH_2CO_2H$, and formic acid[6] have been determined before with the same spectroscopy cells and hydrothermal conditions. The sodium salts of these acids were prepared by adding one equivalent of NaOH to the acid. Solutions were made from Milli-Q water that had been sparged with Ar to remove atmospheric gases.

A Nicolet 60SX FTIR spectrometer with an MCT-B detector was used for the transmission IR spectroscopy experiments. Kinetic measurements in real-time were recorded at 4 cm^{-1} on 32 summed spectra. The total collection time for the summed spectra was approximately 10 s. In all cases the IR spectra were normalized with background spectra of pure H_2O recorded at the same conditions.

The absorptivity of the asymmetric stretch (υ_3) of aqueous CO_2 at 2343 cm^{-1} was used as a real-time diagnostic of the rate of decarboxylation of the compounds. In previous work we have determined the absorptivity of CO_2 in H_2O as a function of temperature,[23] which makes it possible to convert the band area into the concentration. The band area was determined by fitting with a four-parameter Voigt function (Peakfit, Jandel Scientific). Three sets of experimental data were collected in all cases and were averaged to provide the CO_2 concentrations. A weighted least-squares regression was then performed in which the statistical weight, ω_t, was $1/\sigma^2$, where σ is the standard deviation of the concentrations at each time t. Where necessary, ω_t was approximated as $k^2\omega_t$,[26] where k is the rate constant. In the rate constant and Arrhenius analysis, the error limits were translated into log space as $\sigma/\bar{x}$, where $\bar{x}$ is the average CO_2 concentration.[26]

In addition to real-time kinetic measurements, some of the product identities were obtained from postreaction analysis of cooled solutions after reaction in the batch mode. Tubes composed of 316 SS and Ti with an internal volume of 12 cm^3 were sealed with an H_2O solution containing the reactant compound (0.25 m), where m is molal. The loading volume was calculated to be that necessary to fill the tube completely at the reaction temperature under 275 bar pressure. The tube was then inserted into a fluidized sand bath set at the desired temperature and held there for a measured amount of time. After quenching in a water bath, the tube was opened and the solution was analyzed by IR and Raman spectroscopy and/or by GC/mass spectrometry. A short-path-length IR cell with ZnSe windows was used for the IR spectral work. A Kaiser Optical Systems dispersive Raman spectrometer was used to obtain the Raman spectra. It employed a thermomechanically cooled CCD detector and a 50 mW diode-pumped, frequency-doubled, Nd:YAG laser for excitation at 532 nm. The GC/MS data were obtained with an HP 5980 GC with a HP1 column (25 m × 0.25 mm ID) coupled to a HP 5970 series Mass Selective Detector. The flow rate was l mL/min of He.

TABLE 1: Steric Constants, E_s, for R in RCO_2H Compounds

R	this work[a]	literature[b]
CF_3-		−1.16
CCl_3-		−2.06
$HOC(O)CH_2-$	−0.75	
$H_2NC(O)CH_2-$	−1.05	
CF_3CH_2-	−1.1[c]	
$NCCH_2-$	−1.02	−0.94
$CH_3C(O)-$	−0.75	

[a] Determined by the method described in ref 29. [b] Ref 28. [c] Determined by the method described in the text.

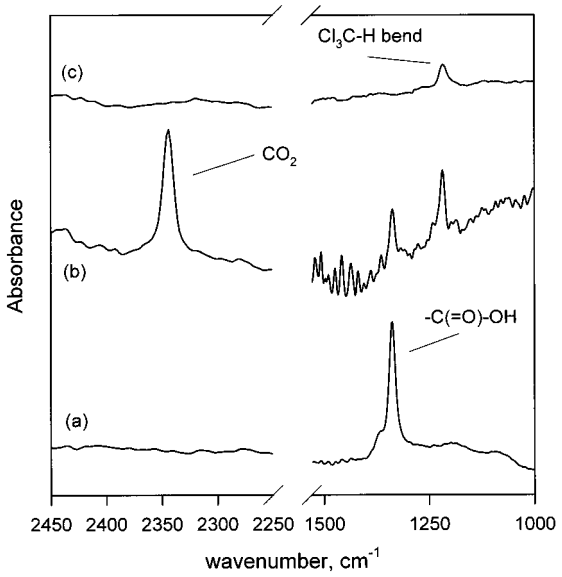

Figure 1. IR spectra of (a) 0.25 *m* CCl_3CO_2H at 25 °C and 1 atm. (b) Solution in (a) cooled to 25 °C after heating for 7.5 min at 130 °C under 275 bar in the Ti tube reaction. (c) An aqueous solution of $CHCl_3$. These spectra validate reaction 2.

The ionization equilibrium constants for the acids were needed for the kinetics analysis. Most are available in standard sources, but pK_a for malonamic acid was not found in a literature search and only one value appears to have been reported for cyanoacetic acid (2.58 at 27 °C).[27] Therefore, pK_a values for these two acids were obtained from the temperature dependence of the pH of aqueous solutions. An Orion 330 pH meter with an Ag/AgCl perpHect electrode calibrated at multiple points by the use of standard buffer solutions was used with the LogR function that corrects for the pH change of H_2O over the temperature range used. The pK_a values of malonamic acid were determined to be 3.59 at 25 °C and 3.55 at 30 °C. pK_a for cyanoacetic acid was 2.48 at 30 °C. These values were used to determine the pK_a values at the higher temperature reaction conditions using the iso-Coulombic method.[28]

For the Taft plot analysis[29] it is necessary to know steric constants, E_s, for R. E_s values are available for many other functional groups,[30] but were not previously reported for R = $NH_2C(O)CH_2-$, HCO_2CH_2-, CF_3CH_2-, and $CH_3C(O)-$ groups. They were determined, therefore, by acid-catalyzed esterification of the carboxylic acid in CH_3OH by *p*-toluenesulfonic acid, as described for other acids.[31] The concentration of the acid catalyst was determined to be 0.0012 M (where M is molar) by titration with standardized NaOH. The rate of esterification was used for comparison with the rate of acetic acid, and cyanoacetic acid was used as the standard to verify that the E_s value obtained matched the previously reported value. Table 1 contains the E_s values used. Trifluoropropionic acid did not react in the esterification attempt so the value of E_s was determined from the van der Waals radius of the CF_3CH_2- group. Comparison of this radius to that of known singly substituted methyl groups[32] provided the values in Table 1. To obtain the Taft parameters δ and ρ,[29] the curve-fitting function of SigmaPlot (Jandel Scientific) was used.

Results and Discussion

Decarboxylation of the Acids. In accordance with several earlier findings,[14,33−37] the decarboxylation of carboxylic acids in H_2O solution was proven spectroscopically to be described, at least initially, by reactions 2−8. These reactions apply to the results in both the SS and Ti cells. In some cases, as discussed below, further reactions of the products occurred.

$$CCl_3CO_2H \rightarrow CHCl_3 + CO_2 \quad (2)$$

$$CF_3CO_2H \rightarrow CHF_3 + CO_2 \quad (3)$$

$$CF_3CH_2CO_2H \rightarrow CF_3CH_3 + CO_2 \quad (4)$$

$$HOC(O)CH_2CO_2H \rightarrow CH_3CO_2H + CO_2 \quad (5)$$

$$NH_2C(O)CH_2CO_2H \rightarrow NH_2C(O)CH_3 + CO_2 \quad (6)$$

$$NCCH_2CO_2H \rightarrow CH_3CN + CO_2 \quad (7)$$

$$CH_3C(O)CO_2H \rightarrow CH_3C(O)H + CO_2 \quad (8)$$

Validations of reactions 2−8 were achieved by the use of IR spectroscopy during the flow reaction, and by IR spectroscopy, Raman spectroscopy, and/or GC−mass spectrometry from the batch reaction mode following cooling and depressurization. CHF_3, $CHCl_3$, and CF_3CH_3 were confirmed by GC-MS and IR spectroscopy to be the only halocarbon products initially formed in reactions 2−4. Figure 1 illustrates the results for 0.25 *m* CCl_3CO_2H which had been heated in a SS tube reactor at 130 °C for 7.5 min at 275 bar. Partial conversion occurred forming $CHCl_3$ which was identified by the IR spectrum of an authentic sample of $CHCl_3$ dissolved in H_2O. When the solution was heated for a longer time or at a higher temperature, partial decomposition of $CHCl_3$ resulted in the formation of additional products. For example, small amounts of CH_2Cl_2 and Cl^- could be detected and were also detected upon heating an authentic solution of $CHCl_3$ in H_2O. The details of this reaction in the SS tube were not investigated further owing to the well-known reactivity of SS in the presence of Cl^- ions.

Reaction 5 has been confirmed previously at hydrothermal conditions by real-time IR spectroscopy, in situ, with 316 SS, Ti, and 90/10 Pt/Ir flow cells.[6,16] Support for reaction 6 was obtained from the Raman spectrum of 1.0 *m* malonamic acid that had been heated at 150 °C for 20 min under 275 bar in a SS tube reactor. By comparison with Raman spectra of authentic samples, Figure 2 reveals that only acetamide and CO_2 are formed. Reaction 7 was confirmed in real-time by IR spectroscopy in the flow reaction mode because the reactant acid and both of the products have IR-active modes in the band-pass of the sapphire windows. This is illustrated in Figure 3 showing the IR spectrum of 1.0 *m* $NCCH_2CO_2H$ at 220 °C under 275 bar and at several residence times in the 316 SS cell. The −CN stretch in both the reactant and product has relatively low absorptivity compared to CO_2, but they can still be detected as the reaction progresses. The gradual shift of the −CN stretch from 2265 cm^{-1} in $NCCH_2CO_2H$ to 2256 cm^{-1} in CH_3CN is observed.

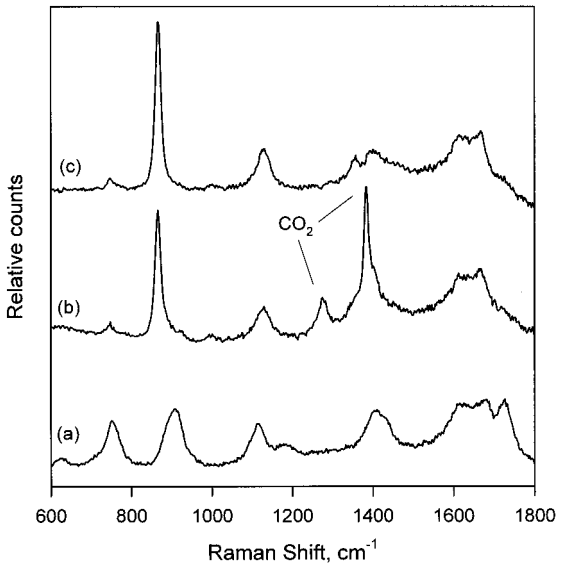

Figure 2. Raman spectra of (a) 1.00 *m* $NH_2C(O)CH_2CO_2H$ (malonamic acid) at 25 °C and 1 atm. (b) Solution in (a) cooled to 25 °C after heating for 20 min at 150 °C under 275 bar in the Ti tube reactor. (c) An aqueous solution of $NH_2C(O)CH_3$. Reaction 6 is indicated.

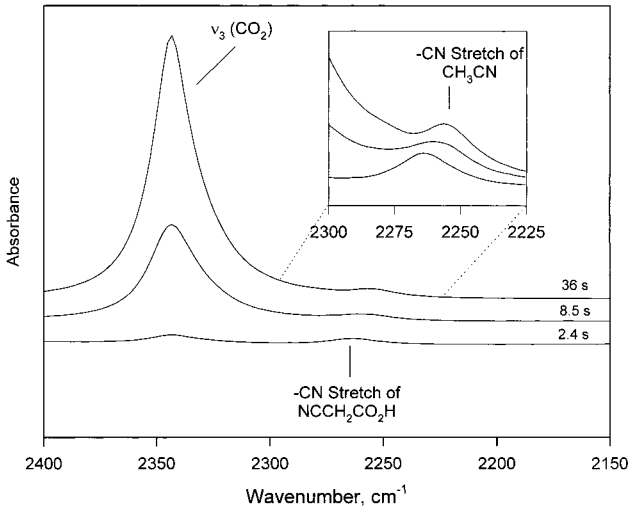

Figure 3. Selected real-time IR spectra of l.00 *m* $NCCH_2CO_2H$ as a function of residence time at 220 °C and 275 bar in the 316 SS flow cell. Conversion according to reaction 7 is revealed.

The products of reaction 8 were found by GC/MS to be primarily acetic acid and CO_2 rather than acetaldehyde and CO_2. In general, aldehydes tend to be absent from the products of hydrothermal reactions owing to their rapid rate of hydrolysis.[38]

Rates of Reactions 2−8. The rate constants for all of the reactions in this article were obtained from the conversion of the peak area of CO_2 into the concentration of CO_2 at each time and temperature.[23] On the basis of previous studies, the rates of reactions 2−8 appear to be much faster in H_2O solution than in the gas phase without the presence of a solvent or the influence of the reactor wall. This fact is reflected in comparing the Arrhenius activation energies, E_a, for both conditions. For example, reaction 3 as a unimolecular process in the gas phase is proposed to have $E_a = 365$ kJ/mol[39] and 96 kJ/mol on a stainless steel reactor wall,[40] as opposed to 176 ± 2 kJ/mol in ethylene glycol solution.[41] Values of 192 and 150 kJ/mol were obtained in this work (vide infra) in H_2O solution at hydrothermal reaction conditions in 316 SS and Ti cells, respectively. We can conclude from these comparisons that the solvent field strongly facilitates the decarboxylation reaction, with structure I having been previously cited as mainly responsible.[10,20] Although the specific structures are not elucidated here, the solvent field probably associates with and polarizes the reactant molecule which contributes to the decarboxylation rate by facilitating H-atom transfer. In addition, the reactor surface might play a role in the rate of reactions 2−8 at hydrothermal conditions. As noted in the Experimental Section, this factor was possible to explore by changing the reactor surface material, but that changing the surface-to-volume ratio was not practical. It was found that the material of construction played a lesser role in the reaction rate compared to that of the R group and so the interpretation was mainly directed at the relative rates of reactions 2−8 in the single-phase hydrothermal medium.

The rate of CO_2 formation was used here to determine the rate of decarboxylation of the acid; however, two sources of CO_2 exist in solution. These are reactions 1 and 9, the latter of which arises as a result of the ionization equilibrium of RCO_2H in H_2O, reaction 10. The temperature dependence of reaction 10 was established by the use of the iso-Coulombic method.[27]

$$RCO_2^- + H_2O \xrightarrow{k_2} RH + CO_2 + OH^- \qquad (9)$$

$$RCO_2H + H_2O \overset{K_a}{\rightleftharpoons} RCO_2^- + H_3O^+ \qquad (10)$$

The values of k_2 were determined for each anion as the Na^+ salt and are discussed later in this article. In determining k_2, hydrolysis of the anion back to the acid form was considered to be negligible based on the iso-Coulombic extrapolation. For example, the concentration of malonic acid was about 10^{-5} that of the acid at 200 °C. CO_2 and OH^- remain ionized in eq 9 to the extent (by calculation) that the HCO_3^- concentration is $\leq 10^{-4}$ that of CO_2. The first-order rate expression for reaction 1, where k_1 is the rate constant, can thus be derived by combining the rate expressions for reactions 1, 9, and 10. The resulting expression is eq 11. Equation 11 takes into account the ionization equilibrium of the acid so that the concentration of the anion is known at all times. The separate kinetic measurements of the rate of decarboxylation of the anion alone provide k_2. This enables the amount of CO_2 produced by the anion to be separated from that from the acid when determining the total CO_2 concentration. Hence, a plot of the right-hand side of eq 11 at each time versus time provides k_1. Equation 11

$$-k_1 t = \ln\left[1 - \frac{[CO_2]_t - [RCO_2^-]_0\,[1 - \exp(-k_2 t)]}{[RCO_2H]_0}\right] \qquad (11)$$

applies at the intrinsic pH of the reaction. However, the addition of 0.3 N HCl to solutions of malonic, malonamic, and trichloroacetic acids did not alter the decarboxylation rate within the error of the measurement.

The temperature range over which the rate constants for reactions 2−8 were derived was determined by the flow rates that are compatible with the reactor. Figure 4 shows the rate plot constructed for $NCCH_2CO_2H$ when the expression on the right-hand side of eq 11 is plotted at each residence time, *t*. These values of time were obtained from the ratio of the cell volume and the flow rate. Most of the rate measurements were taken at ≤40% conversion which permitted plug-flow conditions to be assumed. A disadvantage of using this low degree of conversion is that the order of the reaction is not firmly established, but these reactions are generally agreed to be first-order.[6,7,14−16] Table 2 is a compilation of the rate constants for all of the acids and their anions in the Ti and SS cells. Attention

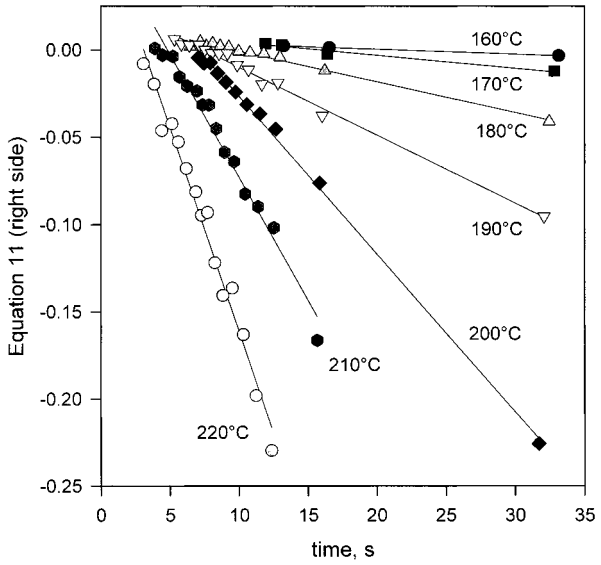

Figure 4. Rate plots for decarboxylation of 0.25 *m* $NCCH_2CO_2H$ in the Ti flow cell under 275 bar pressure. The validity of a first-order rate expression is suggested by the linearity.

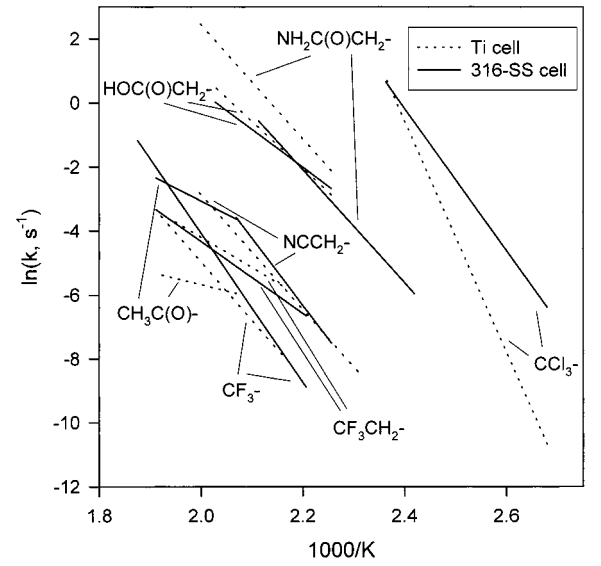

Figure 5. Arrhenius plots showing least-squares fit lines of the decarboxylation rates (Table 2) of the carboxylic acids, RCO_2H (R group shown), in the 316 SS cell compared to the Ti cell.

in this section is focused on the acid data. The anion data are discussed in the next section.

The rate data in Table 2 were converted to Arrhenius constants which are compiled in Table 3 for the acids. Because of the dense clustering of data points, Figure 5 shows the Arrhenius plots for the decarboxylation of the acids in the 316 SS and Ti cells in which only the least-squares fit lines rather than the actual experimental data points (Table 2) are shown. The rates are statistically the same for the two materials of construction within the 95% confidence interval when R = CF_3-, CF_3CH_2-, $NH_2C(O)CH_2-$, and $HOC(O)CH_2-$, and the 90% confidence interval for R = $NCCH_2-$. By comparison, larger differences exist in the decarboxylation rates of formic[6] and acetic acids[8,11] on SS and Ti surfaces. A possible explanation for the larger difference in rates for trichloroacetic acid is the fact that some corrosion occurred in the SS cell, probably as a result of the forementioned reaction with the decomposition products of the CCl_3- group. The Arrhenius parameters for CCl_3CO_2H in the Ti cell also defy a straightforward explanation.

TABLE 2: First-Order Rate Constants for Decarboxylation of Acetic Acid Derivatives and their Anions under 275 bar

	k_1(acid), $s^{-1} \times 10^3$		k_2(anion), $s^{-1} \times 10^3$	
T, °C	316-SS	Ti	316-SS	Ti
	0.25 *m* Cyanoacetic Acid			
140			0.058 ± 0.34	
150			1.9 ± 1.0	1.1 ± 0.6
160		0.29 ± 0.02	3.3 ± 2.6	1.5 ± 0.7
170		0.90 ± 0.42	9.4 ± 5.4	2.8 ± 1.2
180	1.8 ± 0.8	2.5 ± 0.9	18 ± 8	5.7 ± 2.1
190	4.6 ± 1.5	4.7 ± 1.0	33 ± 6	10 ± 4
200	12 ± 2	7.9 ± 1.5	62 ± 8	18 ± 7
210	31 ± 3	19 ± 3		33 ± 3
220		27 ± 3		
	0.25 *m* Malonamic Acid			
140	2.7 ± 0.3	3.5 ± 0.3		
150	11 ± 1	10 ± 1		
160	16 ± 10	27 ± 3		2.1 ± 0.6
170	44 ± 11	80 ± 8		2.2 ± 0.4
180	71 ± 10	170 ± 20	2.5 ± 1.9	2.9 ± 0.3
190	300 ± 140	370 ± 30	2.1 ± 0.3	3.7 ± 0.9
200	520 ± 60		3.7 ± 0.5	5.7 ± 1.1
210			5.3 ± 0.2	7.2 ± 2.1
220			10 ± 2	8.5 ± 1.7
230			12 ± 1	
	0.25 *m* Trichloroacetic Acid			
100	1.3 ± 0.1			
110	9.3 ± 3.0	0.17 ± 0.01	14 ± 7	19 ± 8
120	36 ± 6	6.1 ± 0.3	16 ± 3	39 ± 15
130	160 ± 50	39 ± 20	29 ± 5	53 ± 14
140	430 ± 230	180 ± 70	52 ± 8	75 ± 11
150	330 ± 50		93 ± 15	150 ± 20
	0.25 *m* Trifluoroacetic Acid			
180	0.18			
190	0.50 ± 0.13		1.1 ± 0.4	
200	2.1 ± 1.3		1.7 ± 0.6	
210	4.1 ± 2.1	1.3 ± 0.7	6.7 ± 1.7	1.3 ± 0.6
220	8.9 ± 3.0	5.0 ± 1.7	17 ± 4	5.0 ± 1.8
230	20 ± 8	9.7 ± 3.0	35 ± 9	9.7 ± 3.0
240	66 ± 4	17 ± 4		17 ± 4
250	230 ± 210	34 ± 5		34 ± 5
	0.25 *m* Trifluoropropionic Acid			
190	2.5 ± 1.9	3.1	30 ± 20	
200	4.5 ± 3.2	12	44 ± 30	
210	5.3 ± 3.5	15	64 ± 40	
220	10 ± 7		87 ± 50	
230	16 ± 8		120 ± 70	
240	27 ± 10		130 ± 70	
250			170 ± 90	
260			270 ± 130	
	1.0 *m* Pyruvic Acid			
200	24.1			
210	38.7	2.7	2.3	
220	57	3.1	3.5	0.69
230	71.5	3.7	4.8	0.81
240		4.3	6.6	1.1

Although corrosion was not apparent in the case of pyruvic acid, the rapid decomposition reaction of acetaldehyde in H_2O mentioned above casts uncertainty on reaction 8 as a complete description of the decarboxylation process. On the other hand, reactions 3−7 for the remaining acids do not appear to depend as strongly on whether the cell wall is 316 SS or Ti in the temperature ranges used here, as they do on the functional group R attached to $-CO_2H$. The influence of R on the rate will be discussed below.

Decarboxylation of the Anions. Reactions 2−8 for the protonated form the carboxylate group can be rewritten in terms of the anions according to reaction 9. By applying the same experimental methods as used for the acids, the products of the anions were confirmed to be the same as those in reactions 2−8.

TABLE 3: Arrhenius Parameters for Decarboxylation of Aqueous Solutions of RCO_2H at $T > 100$ °C under 275 bar

		316-SS cell			Ti cell		
compound	σ^* [a]	E_a, kJ/mol	ln(A, s^{-1})	$\Delta S^‡$, J/K·mol at 200 °C	E_a, kJ/mol	ln(A, s^{-1})	$\Delta S^‡$, J/K·mol at 200 °C
CF_3-	2.61	192 ± 5	42.5 ± 1.1	96	151 ± 11	31.5 ± 2.6	4.8
CCl_3-	2.65	184 ± 9	53.3 ± 2.7	190	300 ± 40	86.5 ± 12.1	460
$HOC(O)CH_2-$	1.08	97.9 ± 5.0[b]	24.0 ± 1.3[b]	−57	121 ± 7[b]	30.3 ± 0.1[b]	−5.5
$H_2NC(O)CH_2-$	0.31	146 ± 9	36.7 ± 2.6	48	147 ± 3	38.0 ± 0.8	58
CF_3CH_2-	0.87	92.7 ± 5.3	18.1 ± 1.3	−110	78.6 ± 8.3	14.8 ± 2.1	−130
$NCCH_2-$	1.3	173 ± 2	39.8 ± 0.6	74	149 ± 10	33.0 ± 2.6	17
$CH_3C(O)-$	1.81	75.3 ± 7.1	12.8 ± 1.7	−150	32.3 ± 1.2	2.1 ± 0.3	−240

[a] Taft electronic substituent parameters from Perrin, D. D.; Dempsey, B.; Serjeant, E. P. *pK_a Prediction for Organic Acids and Bases*; Chapman and Hall: New York, 1981. [b] Ref 16.

TABLE 4: Arrhenius Parameters for Decarboxylation of Aqueous Solutions of $RCO_2^-Na^+$ at $T > 100$ °C under 275 bar

	316-SS cell			Ti cell		
R	E_a, kJ/mol	ln(A, s^{-1})	$\Delta S^‡$, J/K·mol at 200 °C	E_a, kJ/mol	ln(A, s^{-1})	$\Delta S^‡$, J/K·mol at 200 °C
CF_3-	178 ± 14	39.6 ± 3.6	72	128 ± 11	26.3 ± 2.5	−38
CCl_3-	65.7 ± 4.5	16.3 ± 1.3	−120	67.7 ± 7.3	17.3 ± 2.1	−110
$HOC(O)CH_2-$	117 ± 5[a]	28.3 ± 1.5[a]	−21	113 ± 2[a]	27.1 ± 0.5[a]	−31
$H_2NC(O)CH_2-$	80.9 ± 5.2	15.0 ± 1.3	−130	45.6 ± 3.7	6.4 ± 0.9	−200
CF_3CH_2-	62.1 ± 2.4	12.7 ± 0.6	−150			
$NCCH_2-$	120 ± 3.4	27.8 ± 0.9	−26	103 ± 3	22.5 ± 0.9	−70
$CH_3C(O)-$	71.5 ± 2.8	11.8 ± 0.7	−160	48.8 ± 9.4	4.6 ± 2.3	−220

[a] Ref 16.

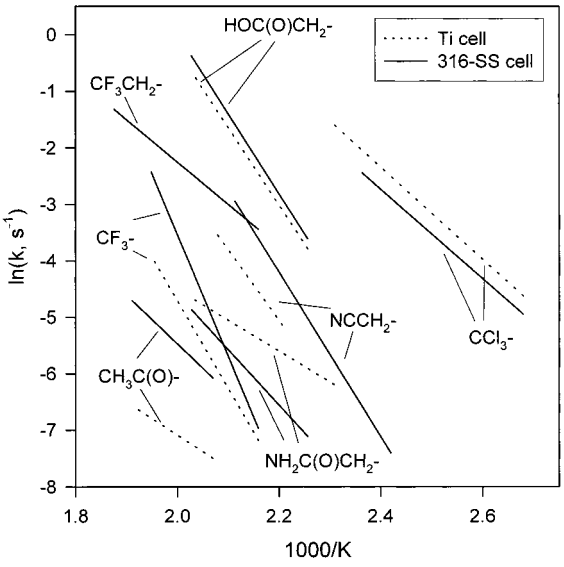

Figure 6. Arrhenius plots showing least-squares fits of the decarboxylation rates (Table 2) of the sodium carboxylate salts, RCO_2Na (R group shown), in the 316 SS cell compared to the Ti cell.

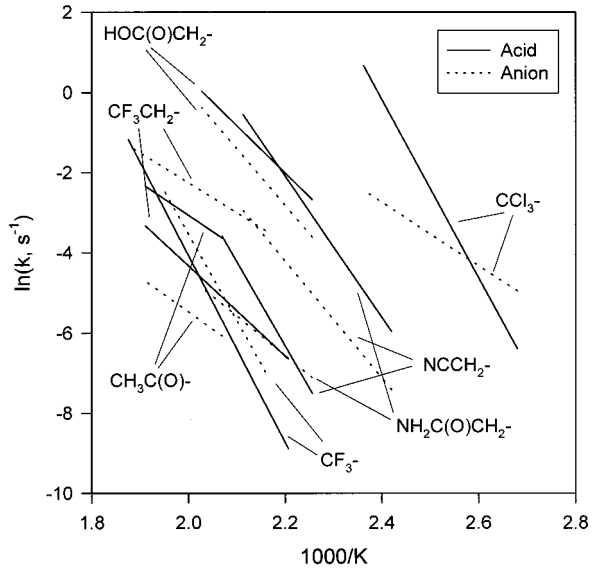

Figure 7. Arrhenius plots comparing the rates least-squares fit lines of the decarboxylation rates of the acids to the anions (Table 2) in the 316 SS cell.

The main difference is that participation of H_2O is required for the stoichiometry and charge balance.

Table 2 gives the rate constants determined in the SS and Ti cells for the sodium carboxylate salts. Table 4 gives the Arrhenius parameters. Figure 6 is the Arrhenius plot showing only least-squares fit lines in order to compare the rates in the two cells. The data are the same within the 95% confidence interval for the trihalo and malonic acids, slightly outside this interval for the cyanoacetic acid, and quite different for malonamic and pyruvic acids. In general, therefore, the material of cell construction has a somewhat larger effect on the decarboxylation rate of the anions than the acids, perhaps because it may be easier for the anions to associate with the metal surface. The functional group R affects the rate the most, however, as will be discussed further in the next section.

It is informative to compare the rate constants for the acids and the anions having the same R group in Table 2. A known fact is that the rate of decarboxylation of the anion is sometimes faster and sometimes slower than that of the acid.[10] According to Table 2 this result is apparent in the present study. For more easy comparison, the Arrhenius data for the acids and anions are plotted together for the SS cell and Ti cell in Figures 7 and 8, respectively. For the keto functional groups (R = $CH_3C(O)-$, $HOC(O)CH_2-$, and $NH_2C(O)CH_2-$), the anions all decarboxylate more slowly than the neutral acid in the temperature range of study. For the nonketo derivatives (R= CCl_3-, CF_3-, $NCCH_2-$, and CF_3CH_2-) the rate of decarboxylation of the anions is faster than that of the corresponding acids. In the case of CCl_3CO_2H this statement is true only in the lower temperature range of the study.

A plausible explanation for the stability of the anionic form of the α- and β-keto acids is the delocalization of charge that is achieved through partial resonance structures. The halo derivatives of acetic acid, on the other hand, will benefit less

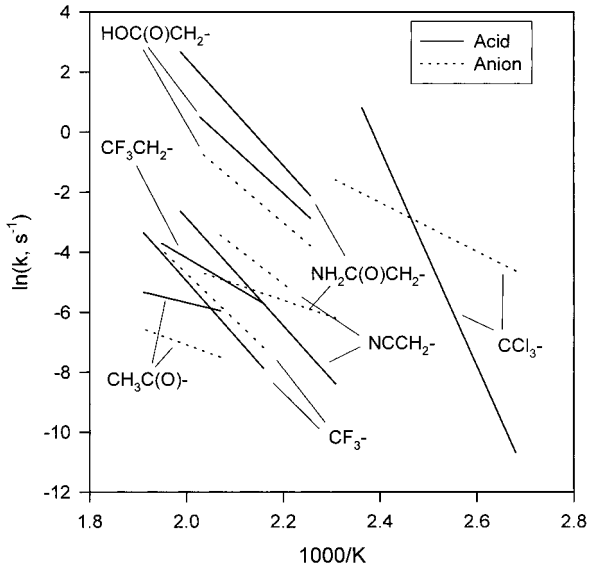

Figure 8. Arrhenius plots of the least-squares fit lines for the decarboxylation rates (Table 2) of the acids compared to the anions in the Ti cell.

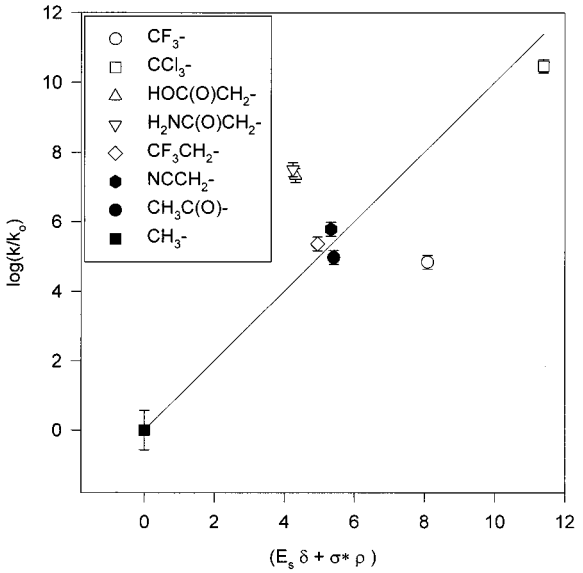

Figure 9. A Taft plot (eq 12) for the decarboxylation rate of the acids at 200 °C in the 316 SS cell.

from this effect and will depend mainly on the electron-withdrawing ability of the halo functional group to stabilize the negative charge on the anion. This latter method is apparently less effective than resonance to stabilize the negative charge.

The more important role of H_2O in the decarboxylation kinetics of the anion (reaction 9) compared to the acid (reaction 1) is manifested in the lower values of $\Delta S^{\ddagger}$ (entropy of activation) in Table 4 compared to Table 3. The only exceptions are malonic acid in the SS cell and pyruvic acid where the $\Delta S^{\ddagger}$ values are similar. The more negative values of $\Delta S^{\ddagger}$ for most of the anions are consistent[42] with the bimolecular form of reaction 9 compared to reaction 1.

Effect of the Functional Group R on the Kinetics. If the mechanism of decarboxylation of these derivatives of acetic acid is the same in all cases, then electron-withdrawing groups would be expected to weaken the C−C bond and facilitate the reaction at a rate that parallels the electron-withdrawing power of R.[10] A correlation between substituent parameters, such as the σ^* parameter of Taft,[30] and E_a or the rates at a given temperature would be expected to exist. Comparison of these substituent parameters in Table 3 and the Arrhenius parameters (Tables 3 and 4) or the rates (Table 2) reveals the absence of any such correlation. Two plausible explanations are that the mechanisms of decarboxylation of these acetic acid derivatives differ when R is varied and/or that the rates are not solely determined by the electron-withdrawing power of R.

Further insight into the possible controlling factors of the homogeneous component of reactions 2−8 was gained by constructing a Taft plot.[29,30] This method helps reveal similarities, differences, and controlling features in the reaction mechanism of closely related compounds. A steric and electronic parameter is employed for each substituent. In the present work it was necessary to determine the steric constants, E_s, for $HOC(O)CH_2-$, $NH_2C(O)CH_2-$, CF_3CH_2-, and $CH_3C(O)-$ to use in conjunction with the known electronic constants, σ^*. The values used are given in Table 1. If the rates are influenced by a combination of steric and electronic parameters of R and the mechanism is similar, then the weighted sum (eq 12) can be optimized in relation to k at a given temperature. To reduce the influence of other variables, such as the solvent effect, the rates were normalized to the rate, k_o, of the reference compound, acetic acid.

$$\log(k/k_o) = \delta E_s + \rho\sigma^* \qquad (12)$$

Figure 9 shows the Taft plot for the decarboxylation rates at 200 °C and 275 bar in the 316 SS cell normalized by the rate of aqueous acetic acid given by Meyer et al.,[9] (E_a = 93 kJ/mol, $\ln(A, s^{-1}) = 10.1$). The particular rate constant chosen for acetic acid merely shifts the ordinate and does not change the overall appearance of the plot. It is apparent that four of the substituents ($R = CH_3C(O)-$, $NCCH_2-$, CF_3CH_2-, and CCl_3-) regress relatively linearly along with $R = CH_3-$, which suggests that their rate of decarboxylation is controlled mainly by a combination of steric and electronic factors of R discussed below. Of the remaining three compounds, two exhibit faster rates than expected ($R = HOC(O)CH_2-$ and $NH_2C(O)CH_2-$), whereas $R = CF_3-$ is slower than expected. The mechanism of decarboxylation of these three derivatives is, therefore, probably somewhat different from the linearly related set in Figure 9. The details of the structures of these compounds offer some insights.

The steric and electronic weighting factors, δ and ρ, respectively, for the linearly related set of compounds in Figure 9 regress to $\rho = 1.5$ and $\delta = -3.6$. The absolute value of ρ and δ indicates the relative weights of the electronic and steric effects of R. The fact that $|\delta|$ is larger than $|\rho|$ implies that the steric effect of R influences the decarboxylation rate somewhat more than the electron-withdrawing effect. More specifically, the rate of decarboxylation increases as the substituent becomes more electron withdrawing and more bulky in the linearly related set, but the steric effect is somewhat more important. Both of these intramolecular effects affect the ease of cleavage of the C−C bond in the parent acid. It is reasonable to expect that the association of a secondary species, H_2O or the reactor wall or both, contributes to the decarboxylation pathway. This is especially evident in the need to transfer an H atom in reactions 2−8. The fact that the reaction is fastest when the steric bulk of R is the greatest casts some doubt on direct association of H_2O with the electropositive carbon atom of the $-CO_2H$ group (structure I) as the initial driving force in this reaction. The increased bulk of R should impede, rather than favor, this association. On the other hand, the association of the oxygen atoms of the carboxylate group either with the reactor surface

or the H_2O solvent field (or both) would be less affected by the steric bulk of R and more plausibly be the initial driving force in accelerating the rate of decarboxylation. The main influence of R remains the ease of cleaving the C−C bond.

Figure 9 shows that R = $HOC(O)CH_2-$ and $NH_2C(O)CH_2-$ decarboxylate at faster rates than expected for steric and electronic control. This most likely results from the ability to form the six-membered cyclic structure III, which facilitates internal H transfer and CO_2 elimination. These are the only compounds studied that can form structure III. For example, this structure is relatively unimportant when R = CF_3CH_2- because of the weak hydrogen bonding ability of the F atom in a C−F bond.[43]

(IV)

When R = CF_3-, Figure 9 reveals that the rate of decarboxylation is slower than expected from the electronic and steric substituent effects of R alone. The electronic anomalies of the CF_3- group are well-known[44−46] and frequently are interpreted as resulting from the hyperconjugative effect IV. Such an effect would somewhat strengthen the C−C bond relative to that predicted by the Taft parameters and thereby retard the rate of decarboxylation.

Conclusions

The stoichiometries of the decarboxylation reactions of H_2O solutions of most acetic acid derivatives, RCO_2H, where R is electron-withdrawing, are relatively straightforward at the hydrothermal conditions. The presence of the H_2O solvent field greatly facilitates the decarboxylation reaction. In contrast to electron-donating groups (especially R = CH_3-) the rates depend more on R than whether the cell is constructed of 316 SS and Ti. The exceptions are greatest when the possibility of cell corrosion and secondary reactions of the products of decarboxylation exist. An explanation for the greater role of the heterogeneous reaction component when R = H− and CH_3- compared to when R is electron-withdrawing lies in the fact that acetic and formic acids are more inert in H_2O. On the other hand, when R is electron-withdrawing, the acids decarboxylate more rapidly at lower temperature and less surface assistance is needed.

Electron-withdrawing R groups accelerate the decarboxylation reaction, and the mechanistic details appear to depend on the nature of R. Some groups anomalously accelerate the reaction while others anomalously retard it. Hence, a simple general relation does not exist between the decarboxylation rate and the electronic and steric properties of the functional group. The anions, likewise, do not decarboxylate at rates that parallel those of the corresponding acid. The anions of the keto derivatives react more slowly than the acid whereas the reverse is true for the nonketo derivatives. In almost all cases, however, the entropy of activation for decarboxylation is more negative for the anion than for the acid which is consistent with a greater role of H_2O in the decarboxylation of the anion. Thus, while homogeneous and heterogeneous pathways probably compete in determining the decarboxylation rate, electron-withdrawing R groups cause the structure of the acid to retain a strong influence and the homogeneous route becomes more important than the differences caused by the SS and Ti cell types.

Acknowledgment. We are grateful to the Army Research Office (R. W. Shaw, Program Manager) for support of this work on the University Research Initiative Grant DAAL03-92-G-0174.

References and Notes

(1) Lewan, M. D.; Fisher, J. B. in *Organic Acids in Geological Processes*; Pittman, E. D., Lewan, M. D., Eds.; Springer-Verlag: Berlin, 1994; Chapter 4.
(2) Shock, E. L. *Org. Life Evol. Biosphere* **1990**, *20*, 331.
(3) Holgate, R. H.; Meyer, J. C.; Tester, J. W. *AIChE J.* **1995**, *41*, 637; Skaates, J. M.; Briggs, B. A.; Lamparter, R. A.; Baillod, C. R. *Can. J. Chem. Eng.* **1981**, *59*, 517.
(4) Mishra, V. S.; Mahajani, V. V.; Joshi, J. B. *Ind. Eng. Chem. Res.* **1995**, *34*, 2.
(5) Shock, E. L. *Am. J. Sci.* **1995**, *295*, 496.
(6) Maiella, P. G.; Brill, T. B. *J. Phys. Chem. A* **1998**, *102*, 5886.
(7) Yu, J.; Savage, P. E. *Ind. Eng. Chem. Res.* **1998**, *37*, 2.
(8) Bell, J. L. S.; Palmer, D. A.; Barnes, H. L.; Drummond, S. E. *Geochim. Cosmochim. Acta* **1994**, *58*, 4155.
(9) Meyer, J. C.; Marrone, P. A.; Tester, J. W. *AIChE J.* **1995**, *41*, 2108.
(10) Clark, L. W. In *The Chemistry of Carboxylic Acids and Esters. The Chemistry of Functional Groups Series*; Patai, S., Ed.; Wiley: New York, 1969; p 589.
(11) Lundegard, P. D.; Kharaka, Y. K. In *Organic Acids in Geological Processes*; Pittman, E. D., Lewan, M. D., Eds.; Springer-Verlag: Berlin, 1994; Chapter 3.
(12) Shock, E. L. In *Organic Acids in Geological Processes*; Pittman, E. D., Lewan, M. D., Eds.; Springer-Verlag: Berlin, 1994; Chapter 10.
(13) Bell, J. L. S.; Palmer, D. A. in *Organic Acids in Geological Processes*; Pittman, E. D., Lewan, M. D., Eds.; Springer-Verlag: Berlin, 1994; Chapter 9.
(14) Fairclough, R. A. *J. Chem. Soc.* **1938**, 1186.
(15) Hall, G. A., Jr. *J. Am. Chem. Soc.* **1949**, *71*, 2691.
(16) Maiella, P. G.; Brill, T. B. *J. Phys. Chem.* **1996**, *100*, 14352.
(17) Lee, I.; Cho, J. K.; Lee, B. S. *J. Chem. Soc., Perkin Trans. 2* **1998**, 1319.
(18) Bernoulli, A. L.; Wege, W. *Helv. Chim. Acta* **1919**, *2*, 511.
(19) Hall, G. A., Jr. *J. Am. Chem. Soc.* **1949**, *71*, 2691.
(20) Fraenkel, G.; Belford, R. L.; Yankwich, P. E. *J. Am. Chem. Soc.* **1954**, *76*, 15.
(21) Kieke, M. L.; Schoppelrei, J. W.; Brill, T. B. *J. Phys. Chem.* **1996**, *100*, 7455.
(22) Schoppelrei, J. W.; Kieke, M. L.; Wang, X.; Klein, M. T.; Brill, T. B. *J. Phys. Chem.* **1996**, *100*, 14343.
(23) Maiella, P. G.; Schoppelrei, J. W.; Brill, T. B. *Appl. Spectrosc.*, in press.
(24) Belsky, A. J.; Brill, T. B. *J. Phys. Chem. A* **1998**, *102*, 4509.
(25) Galat, A. *J. Am. Chem. Soc.* **1948**, *70*, 2596.
(26) Cvetanovic, R. J.; Singleton, D. L. *Int. J. Chem. Kinet.* **1977**, *9*, 481.
(27) Kortum, G.; Wogel, W.; Andrussow, K. *Dissociation Constants of Organic Acids in Aqueous Solutions*; Butterworths: London, 1961.
(28) Lindsay, W. T. *Proc. Int. Water Conf. Eng. Soc. W. Pa.* **1980**, *41*, 284.
(29) Taft, R. W., Jr. *Steric Effects in Organic Chemistry*; Newman, M. S., Ed.; John Wiley and Sons: New York, 1956.
(30) Unger, S. H.; Hansch, C. *Prog. Phys. Org. Chem.* **1976**, *12*, 91.
(31) MacPhee, J. A.; Panaye, A.; Dubois, J. E. *Tetrahedron* **1978**, *34*, 3553.
(32) Charton, M. *J. Am. Chem. Soc.* **1969**, *91*, 615.
(33) King, J. A. *J. Am. Chem. Soc.* **1947**, *69*, 2738.
(34) Hall, G. A., Jr. *J. Am. Chem. Soc.* **1980**, *72*, 4709.
(35) Hall, G. A., Jr.; Verhoek, F. H. *J. Am. Chem. Soc.* **1947**, *69*, 613.
(36) Yamamoto, S.; Back, R. H. *Can. J. Chem.* **1985**, *65*, 549.
(37) Davis, L. L.; Brower, K. R. *J. Phys. Chem.* **1996**, *100*, 18775.
(38) Townsend, S. H.; Klein, M. T. *Fuel* **1985**, *64*, 635.
(39) Francisco, J. S. *J. Chem. Soc., Faraday Trans.* **1992**, *88*, 3521.
(40) Ashworth, A.; Harrison, P. G. *J. Chem. Soc., Faraday Trans.* **1993**, *89*, 2409.
(41) Auerbach, I.; Verhoek, F. H.; Henne, A. L. *J. Am. Chem. Soc.* **1950**, *72*, 299.
(42) Conners, K. A. *Chemical Kinetics*; VCH: New York, 1990; p 220.
(43) West, R.; Powell, D. L.; Whately, L. S.; Lee, M. K. T.; Schleyer, P. von R. *J. Am. Chem. Soc.* **1962**, *84*, 3221.
(44) Roberts, J. D.; Webb, R. L.; McElhill, E. A. *J. Am. Chem. Soc.* **1955**, *72*, 408.
(45) Koppel, I. A.; Pihl, V.; Koppel, J.; Anvia, F.; Taft, R. W. *J. Am. Chem. Soc.* **1994**, *116*, 8654.
(46) Paleta, O. *Chem. Listy* **1970**, *64*, 366.